13_040220_CLN_01.doc

TO: DISTRIBUTION
FROM: C NEUMEYER
SUBJECT: ANALYSIS OF TF COMMISSIONING ISTP RESULTS

This memo serves to document the TF-related results of ISTP-001 conducted between 1/16 and 1/20/4 to commission the new TF coil system and to restart NSTX. In addition it discusses the rationale for the present TF operating envelope of 4.5kG/1.0 second and outlines plans for follow-on work required to justify higher operating levels.

TF shots in the ISTP-001 Test Plan consisted of four TF-only shots at increasing levels which imposed equal increments of in-plane EM load and approximately equal increments of $\int i^2(t)dt$, followed by two additional test shots which include combined field out-of-plane loads. These latter two shots are representative of plasma operation and form the basis for the combined field 50% and 100% level standard daily test shots. The shots were planned[1] in advance of the ISTP and were analyzed using the FEA models with the aim of comparing predicted quantities to measured quantities as part of the ISTP.

The ISTP test results show areas of agreement with the analytic predictions, but also areas where the measurements do not track the predictions very well. Also, the joint-to-joint variation is larger than anticipated. And, the results are not consistent with the prototype testing in terms of the effect of applied loads on joint resistance. Therefore follow-on activities have been initiated to develop refinements to the analytic model with the aim of benchmarking it against the measurements. Another round of prototype tests may be performed as well.

In the interim, the operating envelope has been set to allow 4.5kG and a maximum I2T of 3.6e9A2-sec, which represents 56% of the in-plane EM load, 75% of the out-of-plane EM load, and 77% of the maximum thermal load, with respect to the 6kG design basis case.

This envelope is judged to be safe, despite the aforementioned discrepancies, based on the fact that the energy dissipation at the worst case joints is estimated to be of the same order as that allowed for in the analysis of the design basis 6kG pulse. The situation is really far more complex, of course, considering the non-uniform current densities, pressures and conductivities (electrical and thermal) along the joint, along with the time dependencies of the thermal diffusion away from the joint. Nevertheless, an encouraging factor is that stable operation at 4.5kG has been demonstrated.

---

[1] "TF Recommissioning Sequence", 13_031203_CLN_01.doc

But clearly more work needs to be done to develop a reliable predictive model and a better understanding of the behavior. At this time efforts are underway to develop modified FEA models which represent the locality of the joint in greater detail than previously. The expectation is that the greater level of detail will lead to better agreement between the predicted voltage, temperature, and strain measurements, and that the model will still predict acceptable conditions at 6kG.

General Questions To Be Addressed

1) Does measured behavior agree with analytic model?

- How much difference exists between measurements and predictions?
- Does model need to be changed?
- Does operating envelope need to be reconsidered?

2) Do all joints of the same type behave the same way?

- What variation exists joint-to-joint?
- Are any joints significantly different than others?

3) Is behavior changing as more load cycles are applied?

Measurement Details

Voltage across each joint is measured using probes as shown in figure 1 below.

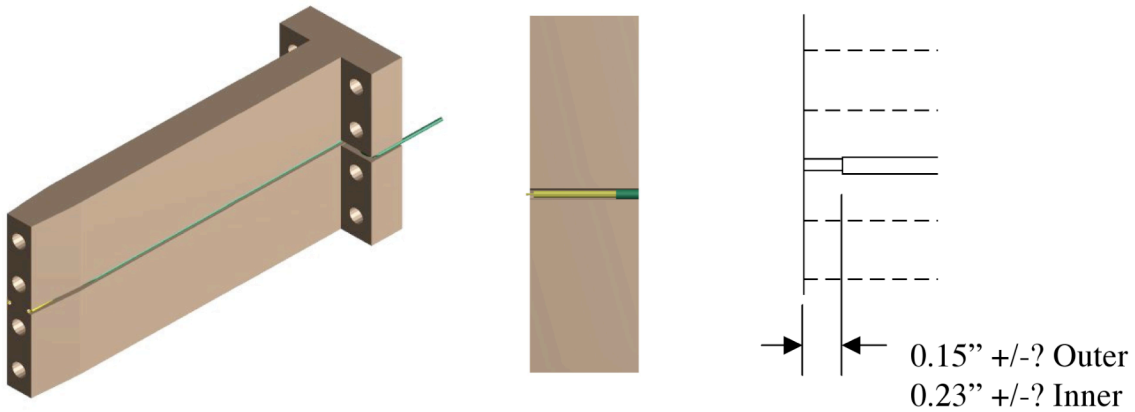

Figure 1 – Voltage Probe Arrangement

Voltage drop necessarily includes bulk resistance effect due to distance over which probe barrel is in contact with copper. Nominal dimensions are shown in the figure. However, due to the final clean-up machining step, the tolerance on this dimension is unknown, and could be quite variable.

Theoretical resistance measurement is based on the following curve showing the effect of contact pressure on contact resistivity.

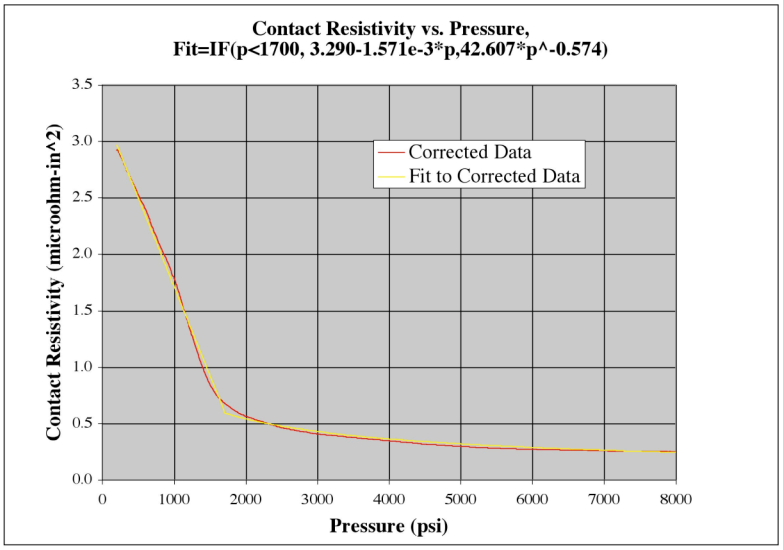

Figure 2 – Contact Resistivity vs. Pressure

On this basis, and the nominal flag stud tension, predicted resistances under no load at 20C are as shown in Table 1.

TABLE 1 – PREDICTED JOINT RESISTANCE VALUES

	Outer Layer, Nominal	Inner Layer, Nominal	
Probe Gap	0.15	0.23	in
Height	5	5	in
Width	0.781	1	in
Hole Dia	0.563	0.563	in
Groove Dia	0.048	0.048	in
Groove Depth	0.142	0.142	in
CSA	2.90	3.99	in^2
20C Bulk Resistance	0.035	0.039	microohm
Force	20000	20000	lbf
Pressure	6906	5011	psi
Contact Resistivity	0.114	0.224	microohm-in^2
Contact Resistance	0.039	0.056	microohm
Temperature(200A)	20	20	C
Bulk Resistance(200A)	0.035	0.039	microohm
Total Resistance(200A)	0.074	0.095	microohm

The above predicts an average resistance of around 75 nano-Ohm (nΩ) for the outer layer flags and 95 nΩ for the inners, whereas the actual measured values[2] following initial installation had averages of 40 nΩ and 75 nΩ. The following figure gives an indication of the kind of variability initially measured.

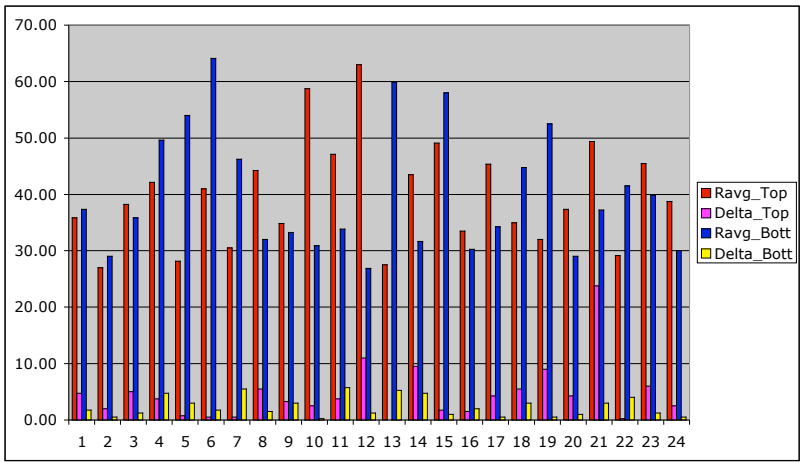

Figure 3 – Outer Flag Joint Resistance (nΩ) vs. Joint Number, Average of "A" and "B" probes, and difference between "A" and "B" probes

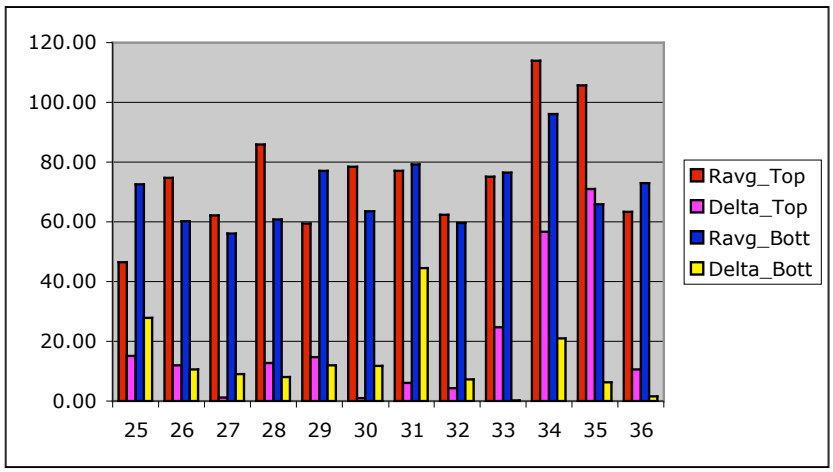

Figure 4 – Outer Flag Joint Resistance (nΩ) vs. Joint Number, Average of "A" and "B" probes, and difference between "A" and "B" probes

[2] TF Joint Measurements by H Schneider and R Marsala 12/12/3

TABLE 2 – FIRST 200A MEASUREMENT
OF JOINT RESISTANCES

Location	nΩ
Ravg_Outer_Top	40
Ravg_Outer_Bott	40
Ravg_Outer	40
Rstdv_Outer	10
Ravg_Inner_Top	75
Ravg_Inner_Bott	70
Ravg_Inner	73
Rstdv_Inner	17

Strain and temperature probes are installed in four flags (2 top (1 inner, 1 outer) and 2 bottom (1 inner and 1 outer) and their shear shoes as indicated in the figure 5.

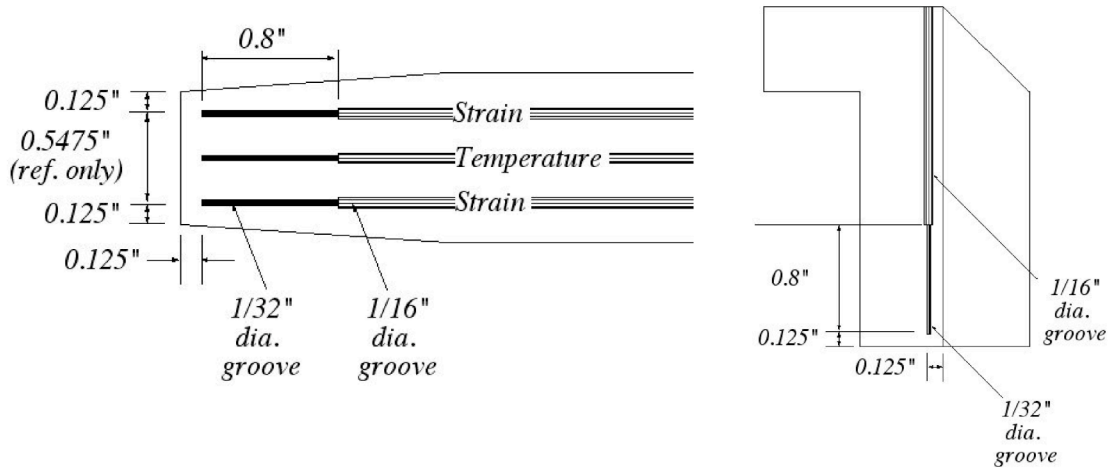

Figure 5 – Contact Resistivity vs. Pressure

It is noted that the temperature probes have an active length of ~ 0.75" and are epoxied into a groove. Per the manufacturer, the time response of the probe time alone is 30mS, but the response in this configuration, with the epoxy, is not known at this time. The range of the probes is 0-150C, and the scale factor is TBD volts/^{o}C (i.e. TBD degrees/volt).

The range of the strain probes is –2500 (compression) to 200 (tension) microstrain. The strain probes have an active length of ~ 0.4" and are also epoxied into grooves.

G-10 rods were affixed to several flag ends and displacement transducers affixed to the umbrella structure to measure the toroidal displacement at the ends of the rods as a measure of the angular twist of the TF bundle. Total radius out to the transducers is TBD inches on outer flags and TBD inches on inner flags, so the scale factor is TBD inch/degree for the outers and TBD inch/degree on the inners. Then, considering that the scale factor of the probe is 10V/inch, the final signal scale factor is TBD volts/degree (i.e. TBD degrees/volt) on the outers and TBD volts/degree (i.e. TBD degrees/volt) on the inners.

One displacement transducer was affixed to the top of the machine to measure the axial displacement of the TF bundle at the spline with respect to the umbrella cover. The scale factor is 10V/inch (i.e. 100mils/volt).

ISTP Shot Summary

Shot list and FISO signal conditioner channel usage is shown in the following table.

TABLE 3 – ISTP SHOT SUMMARY

Shot	Date	Itf (kA)	PF/OH (%)	Comments	FISO#1	FISO#2	FISO#3	FISO#4	FISO#5	FISO#6	FISO#7	FISO#8	19_19 Probes
110752	1/16/04	26.7	0	Analysis Case #1	Top Outer Flag Temp FOE#8	Bot Inner Flag Temp FOE#13	Top Outer Flag Strain FOE#6	Top Outer Flag Strain FOE#7	Bot Inner Flag Strain FOE#14	Bot Inner Flag Strain FOE#12	Top Inner Flag Strain FOE#2	Top Inner Flag Strain FOE#1	TFJ_19_19_V=B
110755	1/16/04	37.8	0	Analysis Case #2	Top Outer Flag Temp FOE#8	Bot Inner Flag Temp FOE#13	Top Outer Flag Strain FOE#6	Top Outer Flag Strain FOE#7	Bot Inner Flag Strain FOE#14	Axial Delta L FOE#19	Top Inner Flag Strain FOE#2	Top Inner Flag Strain FOE#1	TFJ_19_19_V=B
110757	1/16/04	46.2	0	Analysis Case #3	Top Outer Flag Temp FOE#8	Bot Inner Flag Temp FOE#13	Top Outer Flag Strain FOE#6	Top Outer Flag Strain FOE#7	Bot Inner Flag Strain FOE#14	Axial Delta L FOE#19	Top Inner Flag Strain FOE#2	Top Inner Flag Strain FOE#1	TFJ_19_19_V=B
110758	1/16/04	53.4	0	Analysis Case #4	Top Outer Flag Temp FOE#8	Bot Inner Flag Temp FOE#13	Top Outer Flag Strain FOE#6	Top Outer Flag Strain FOE#7	Bot Inner Flag Strain FOE#14	Axial Delta L FOE#19	Top Inner Flag Strain FOE#2	Top Inner Flag Strain FOE#1	TFJ_19_19_V=B
110790	1/19/04	26.7	0	Repeat of Analysis Case #1	Top Outer Flag Temp FOE#8	Top Shear Key Strain FOE#5	Top Outer Flag Strain FOE#6	Top Outer Flag Strain FOE#7	Bot Inner Flag Strain FOE#14	Axial Delta L FOE#19	Top Outer Flag Rotation FOE#17	Bot Inner Flag Rotation FOE#20	TFJ_19_19_V=B
110791	1/19/04	37.8	0	Repeat of Analysis Case #2	Top Outer Flag Temp FOE#8	Top Shear Key Strain FOE#5	Top Outer Flag Strain FOE#6	Top Outer Flag Strain FOE#7	Bot Inner Flag Strain FOE#14	Axial Delta L FOE#19	Top Outer Flag Rotation FOE#17	Bot Inner Flag Rotation FOE#20	TFJ_19_19_V=B
110792	1/19/04	46.2	0	Repeat of Analysis Case #3	Top Outer Flag Temp FOE#8	Top Shear Key Strain FOE#5	Top Outer Flag Strain FOE#6	Top Outer Flag Strain FOE#7	Bot Inner Flag Strain FOE#14	Axial Delta L FOE#19	Top Outer Flag Rotation FOE#17	Bot Inner Flag Rotation FOE#20	TFJ_19_19_V=B
110793	1/19/04	53.4	0	Repeat of Analysis Case #4	Top Outer Flag Temp FOE#8	Top Shear Key Strain FOE#5	Top Outer Flag Strain FOE#6	Top Outer Flag Strain FOE#7	Bot Inner Flag Strain FOE#14	Axial Delta L FOE#19	Top Outer Flag Rotation FOE#17	Bot Inner Flag Rotation FOE#20	TFJ_19_19_V=B
110795	1/20/04	26.7	0	Repeat of Analysis Case #1	Top Outer Flag Temp FOE#8	Top Shear Key Strain FOE#5	Top Outer Flag Strain FOE#6	Top Outer Flag Strain FOE#7	Bot Outer Shear Key Strain FOE#15	Axial Delta L FOE#19	Top Outer Flag Rotation FOE#17	Bot Inner Flag Rotation FOE#20	TFJ_19_19_V=B TFJ_SPARE_01=A
110796	1/20/04	37.8	0	Repeat of Analysis Case #2	Top Outer Flag Temp FOE#8	Top Shear Key Strain FOE#5	Top Outer Flag Strain FOE#6	Top Outer Flag Strain FOE#7	Bot Outer Shear Key Strain FOE#15	Axial Delta L FOE#19	Top Outer Flag Rotation FOE#17	Bot Inner Flag Rotation FOE#20	TFJ_19_19_V=B TFJ_SPARE_01=A
110797	1/20/04	46.2	0	Repeat of Analysis Case #3	Top Outer Flag Temp FOE#8	Top Shear Key Strain FOE#5	Top Outer Flag Strain FOE#6	Top Outer Flag Strain FOE#7	Bot Outer Shear Key Strain FOE#15	Axial Delta L FOE#19	Top Outer Flag Rotation FOE#17	Bot Inner Flag Rotation FOE#20	TFJ_19_19_V=B TFJ_SPARE_01=A
110798	1/20/04	53.4	0	Repeat of Analysis Case #4	Top Outer Flag Temp FOE#8	Top Shear Key Strain FOE#5	Top Outer Flag Strain FOE#6	Top Outer Flag Strain FOE#7	Bot Outer Shear Key Strain FOE#15	Axial Delta L FOE#19	Top Outer Flag Rotation FOE#17	Bot Inner Flag Rotation FOE#20	TFJ_19_19_V=B TFJ_SPARE_01=A
110799	1/20/04	26.7	50	Analysis Case #5	Top Outer Flag Temp FOE#8	Top Shear Key Strain FOE#5	Top Outer Flag Strain FOE#6	Top Outer Flag Strain FOE#7	Bot Outer Shear Key Strain FOE#15	Axial Delta L FOE#19	Top Outer Flag Rotation FOE#17	Bot Inner Flag Rotation FOE#20	TFJ_19_19_V=B TFJ_SPARE_01=A
110803	1/20/04	53.4	100	Analysis Case #6	Top Outer Flag Temp FOE#8	Top Shear Key Strain FOE#5	Top Outer Flag Strain FOE#6	Top Outer Flag Strain FOE#7	Bot Outer Shear Key Strain FOE#15	Axial Delta L FOE#19	Top Outer Flag Rotation FOE#17	Bot Inner Flag Rotation FOE#20	TFJ_19_19_V=B TFJ_SPARE_01=A
					Notes: Changed from TFJ_FISO_CH2 to TFJ_3232SP02 1/20 11:00 am after 110798				Notes: Changed from TFJ_FISO_CH6 to TFJ_3232SP02 1/20 9:00 am after 110793				

FISO Probe Details

FISO probe details are given in the following table.

TABLE 4 – FISO DETAILS

Extension Fiber	Probe	SN	Cal Fac	Range	Units	Location	Top/Bott	Inner/Outer	Box#	Turn#	LH/RH	FISO CH# <= 110790	FISO CH# <= 110795	FISO CH#
3	Temperature	T020506I	4328585	0 to 150	Degree C	Flag	Top	Inner	4	27				
2	Strain		N-1003970	-2500 to 200	Micro Strain	Flag	Top	Inner	4	27	LH	7		
1	Strain		N-1003818	-2500 to 200	Micro Strain	Flag	Top	Inner	4	27	RH	8		
4	Strain		N-1003805	-2500 to 200	Micro Strain	Shoe	Top	Inner	4	27				
18	Displacement		8056624	0 to 150	Mils	Flag	Top	Inner	6	25				
8	Temperature	T020506L	4317553	0 to 150	Degree C	Flag	Top	Outer	10	21		1	1	1
6	Strain		N-1003821	-2500 to 200	Micro Strain	Flag	Top	Outer	10	21	LH	3	3	3
7	Strain		N-1003836	-2500 to 200	Micro Strain	Flag	Top	Outer	10	21	RH	4	4	4
5	Strain		N-1003834	-2500 to 200	Micro Strain	Shoe	Top	Outer	10	21			2	2
17	Displacement	04495F01	8056837	0 to 150	Mils	Flag	Top	Outer	12	23			7	7
13	Temperature	T020519B	4296505	-40to 250	Degree C	Flag	Bott	Inner	4	27		2		
12	Strain	04495A07	N-1003832	-2500 to 200	Micro Strain	Flag	Bott	Inner	4	27	LH	6		
14	Strain	04494A06	N-1003816	-2500 to 200	Micro Strain	Flag	Bott	Inner	4	27	RH	5	5	
15	Strain	04495A05	N-1003873	-2500 to 200	Micro Strain	Shoe	Bott	Inner	4	27				5
20	Displacement		8056581	0 to 150	Mils	Flag	Bott	Inner	12	31			8	8
10	Strain		N-1003791	-2500 to 200	Micro Strain	Shoe	Bott	Outer	10	21				
BROKEN	Strain	04495A04	N-1003759	-2500 to 200	Micro Strain	Flag	Bott	Outer	10	21	LH			
11	Strain		N-1003813	-2500 to 200	Micro Strain	Flag	Bott	Outer	10	21	RH			
9	Temperature	T020506M	4300510	0 to 150	Degree C	Flag	Bott	Outer	10	21				
19	Displacement		8056773	0 to 150	Mils	Spline	Top						6	6

Shot Details and Analysis Predictions

Specifications and shot numbers for the 6 types of test shots is given in the following table.

TABLE 5 – SHOT DETAILS

	Shot	Bt	dT	Tflat	PF	Time	ITF	IOH	IPF1A	IPF1B	IPF2	IPF3	IPF5
1	110795	2.25	11	1	0%	SOFT	26.7	0.0	0.0	0.0	0.0	0.0	0.0
						EOFT	26.7	0.0	0.0	0.0	0.0	0.0	0.0
2	110796	3.18	23	1	0%	SOFT	37.8	0.0	0.0	0.0	0.0	0.0	0.0
						EOFT	37.8	0.0	0.0	0.0	0.0	0.0	0.0
3	110797	3.90	36	1	0%	SOFT	46.2	0.0	0.0	0.0	0.0	0.0	0.0
						EOFT	46.2	0.0	0.0	0.0	0.0	0.0	0.0
4	110798	4.50	50	1	0%	SOFT	53.4	0.0	0.0	0.0	0.0	0.0	0.0
						EOFT	53.4	0.0	0.0	0.0	0.0	0.0	0.0
5	110799	2.25	50	1	50%	SOFT	26.7	-12.0	0.0	0.0	0.0	-2.5	0.0
						OHSS	26.7	12.0	-7.5	0.0	-10.0	10.0	10.0
						EOFT	26.7	0.0	0.0	0.0	0.0	0.0	0.0
6	110803	4.50	50	1	100%	SOFT	53.4	-24.0	0.0	0.0	0.0	-2.5	0.0
						OHSS	53.4	24.0	-15.0	0.0	-10.0	10.0	10.0
						EOFT	53.4	0.0	0.0	0.0	0.0	0.0	0.0

Corresponding analytic predictions are given in the following table.

TABLE 6 – ANALYTIC PREDICTIONS

		#1		#2		#3		#4		#5		#6		
		SOFT	EOFT	SOFT	EOFT	SOFT	EOFT	SOFT	EOFT	SOFT	OHSS	EOFT	SOFT	OHSS	EOFT
Outer Flag	delta T (degC)	0.4	8.1	1.3	16.8	2.7	25.8	4.6	35.5	0.4	5	8.1	4.6	33.2	35.5
	Flag Strain A (μS)	51	133	166	329	290	532	409	716	-220	474	133	-184	809	716
	Flag Strain B (μS)	51	133	166	329	290	532	409	716	455	-165	133	533	-3	716
	Shoe Strain B (μS)	4	6	8	10	11	14	14	14	12	-4	6	15	-11	14
	Twist Angle (deg)	0	0	0	0	0	0	0	0	0.03	0.04	0	0.09	0.1	0
Inner Flag	delta T (degC)	0.1	2.2	0.3	4.5	0.7	7	1.3	9.6	0.1	1.4	2.2	1.3	6.3	9.6
	Flag Strain A (μS)	7	1	13	21	19	31	26	44	-12	30	1	-8	78	44
	Flag Strain B (μS)	7	1	13	21	19	31	26	44	27	-11	1	73	1	44
	Shoe Strain B (μS)	0	0	0	0	0	0	0	0	0	0	0	0	0	0
	Twist Angle (deg)	0	0	0	0	0	0	0	0	0.18	0.25	0	0.27	0.31	0
Axial Expansion	(mils)		35		70		113		156			35			156

TF-Only Shots

The following results focus on the outer layer turn number 21 on the top of the machine which is referred to as 21_21. This is one of the turns which was instrumented with the fiber optic strain and temperature probes. Response of the voltage probes on 21_21 to the four TF-only shots is shown in figure 6.

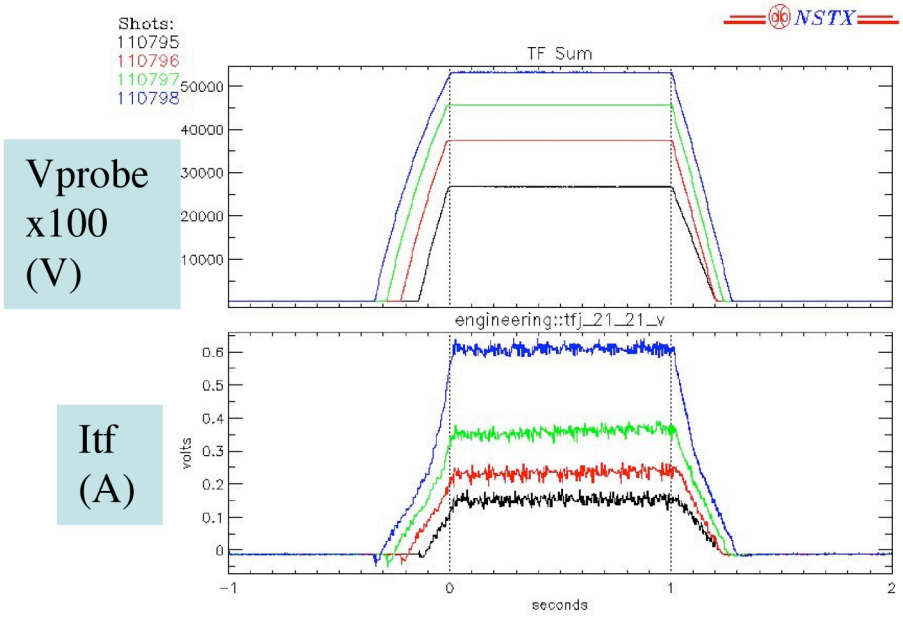

Figure 6 – Voltage Probe Response to In-Plane Loading

Response of the temperature probe on 21_21 to the four TF-only shots is shown in figure 7. The behavior of the last shot (110798) is noticeably different than the others.

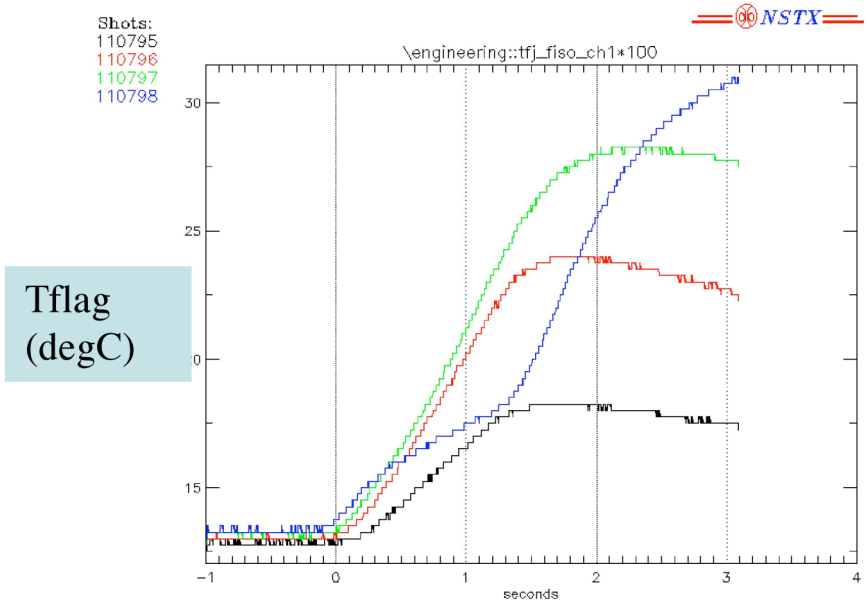

Figure 7 – Temperature Probe Response to In-Plane Loading

The temperature pattern during the pulse (t < 1.2) is counterintuitive, considering that the four pulses have equal increments of $\int i^2(t)dt$. However, the temperatures are noted to redistribute some time after the pulse (t ≥ 2 seconds) into a pattern which follows the $\int i^2(t)dt$.

Response of the flag strain probes on 21_21 to the four TF-only shots is shown in figure 8. Again, the behavior of the last shot (110798) is noticeably different than the others. Also, on the third shot (110797) a difference begins to develop between the strain probes on either side of the joint. Note that strain develops both as a function of the EM loads and of the temperature. After t=1.2 seconds or so, the EM field is off and the remaining strain can be attributed solely to temperature, and the strain level is noted to equalize on the two probes after this time. It is noted, further, that both the EM (in-plane) and thermal loads result in positive strain at this location. So, the most likely explanation for the last shot is that the temperature at the probe location was less (during the pulse) than during the prior shot, which is consistent with the observations in figure 7. One would expect, for pure in-plane loading, that there would be no side-to-side variation but clearly some effect is present here (most noticeably in the third shot (110797).

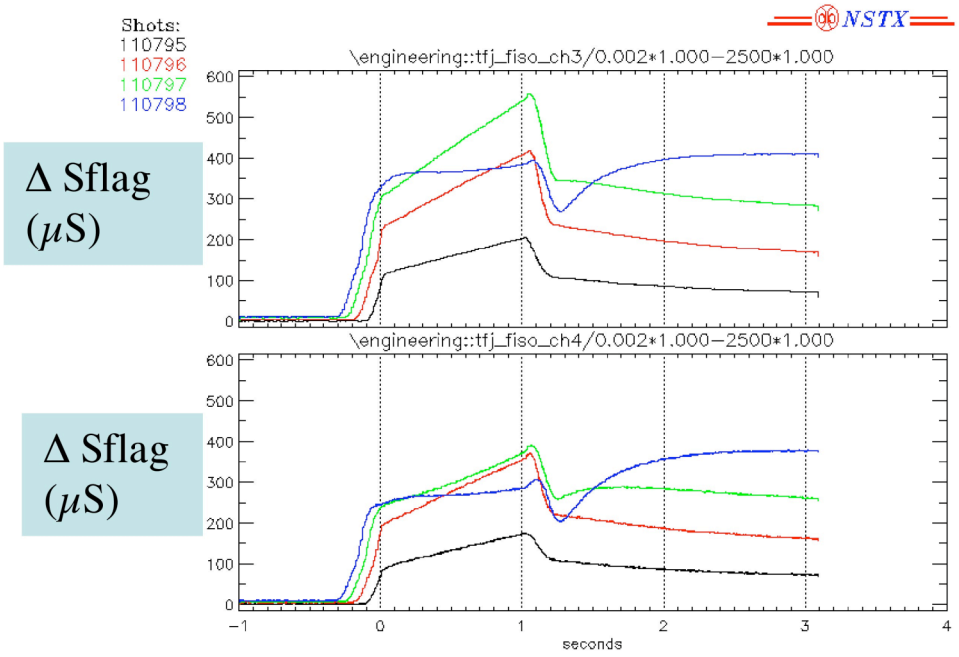

Figure 8 – Flag Strain Probe Response to In-Plane Loading

Response of the shear shoe strain probe on 21_21 to the four TF-only shots is shown in figure 9. Increasing levels of compression are noticeable in the last two shots, which one would expect at the shear shoe begins to pick up load.

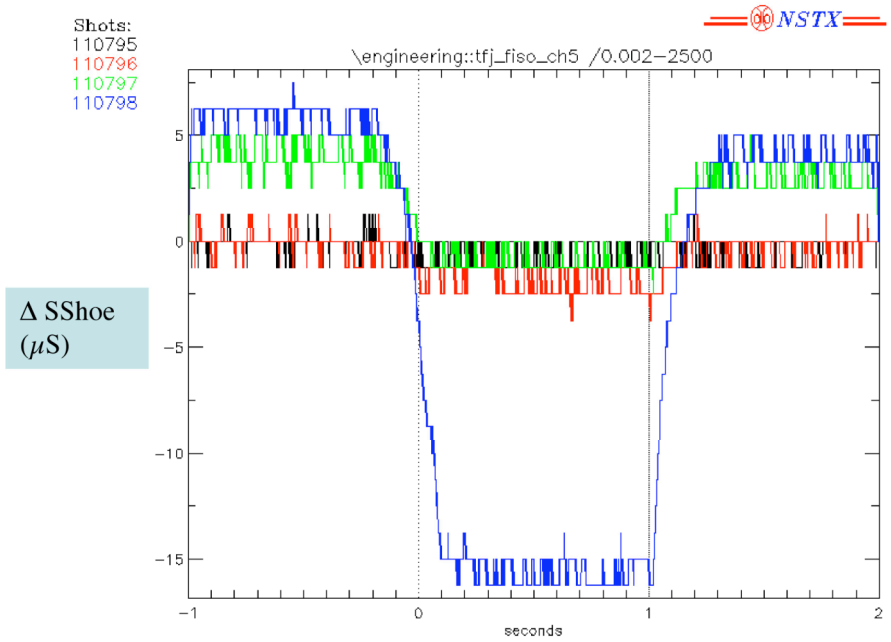

Figure 9 – Shoe Strain Probe Response to In-Plane Loading

Response of the axial displacement probe to the four TF-only shots is shown in figure 10. It is noted that the peaks occur at the end of flat top (t=1.0) and that after the EM load goes away (t ≥ 1.2 seconds) only the thermal effect remains.

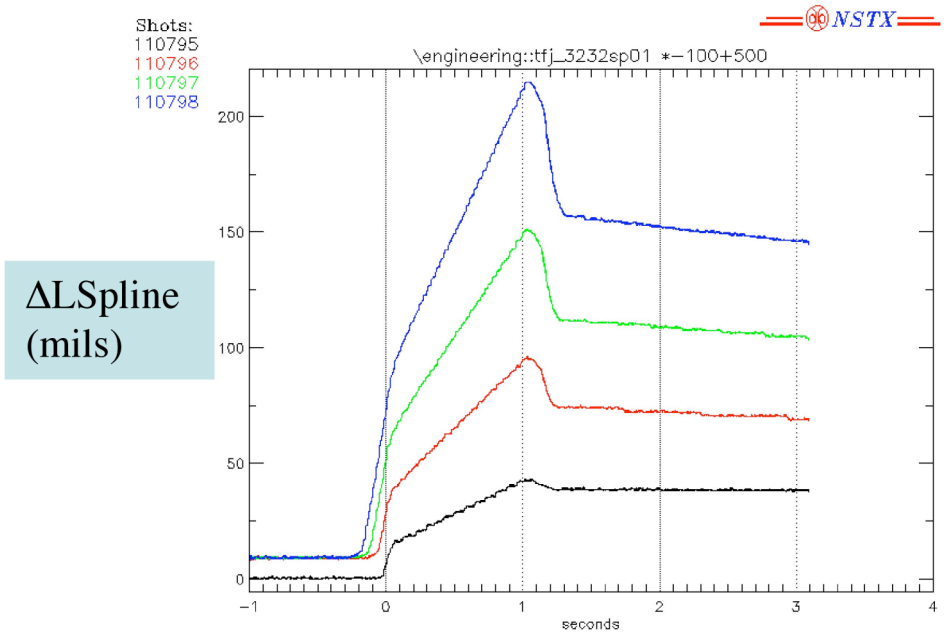

Figure 10 – Shoe Strain Probe Response to In-Plane Loading

Combined Field Shots

Voltage probe response to the two combined field shots (110799:50% and 110803:100%) are shown overlaid with the TF-only shots with the same TF level (110795 and 110798) in figure 11. Also shown are the OH waveforms. Other PF coil waveforms are not shown, but are of less significance. The effect of the OH is clearly evident on the combined field signals.

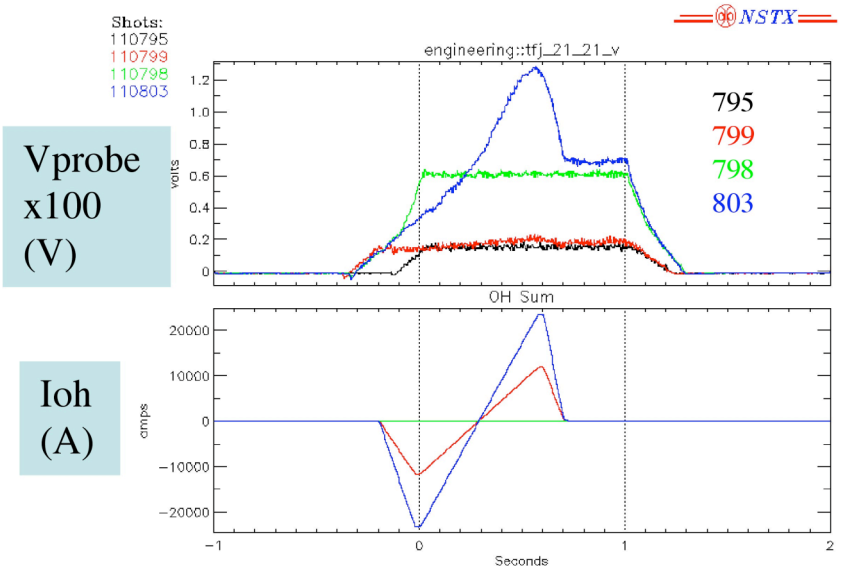

Figure 11 – Voltage Probe Response

Temperature probe response to the two combined field shots are shown overlaid with the TF-only shots with the same TF level in figure 12. No significant difference is noted between the in-plane and out-of-plane cases.

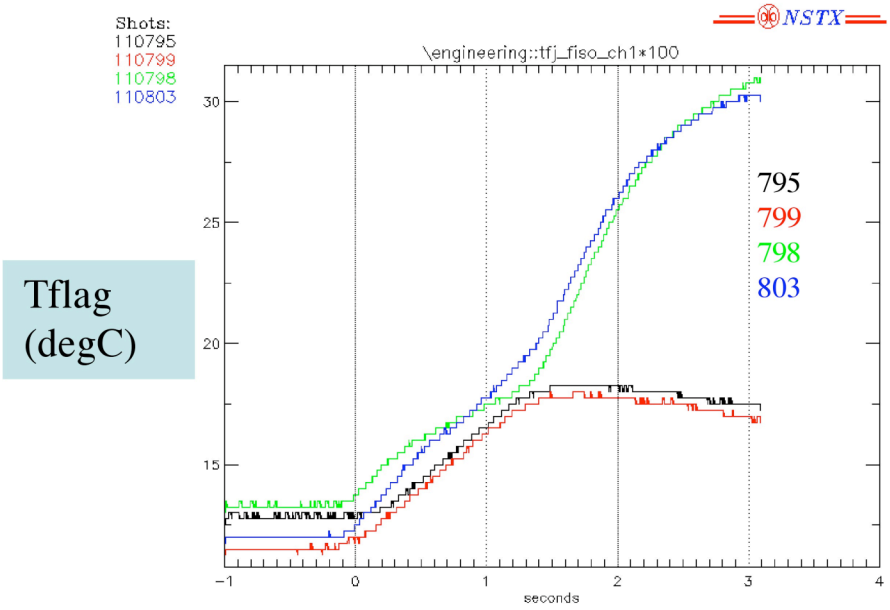

Figure 12 – Temperature Probe Response

Response of the flag strain probes on 21_21 to the combined-field shots is shown in figure 13. The effect of the OH is clearly evident, causing a response which is has an inverse relationship on the two sides of the flag, i.e. when one goes up, the other goes down, and vice-versa.

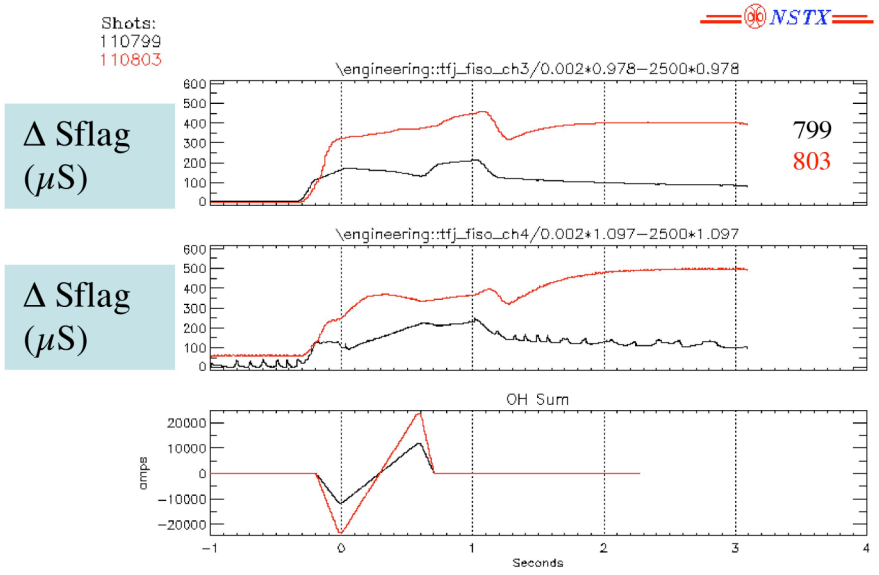

Figure 13 – Flag Strain Response

Response of the shear shoe strain probe on 21_21 to the combined-field shots is shown in figure 14. An increase in the shoe strain at the 100% field level is noted.

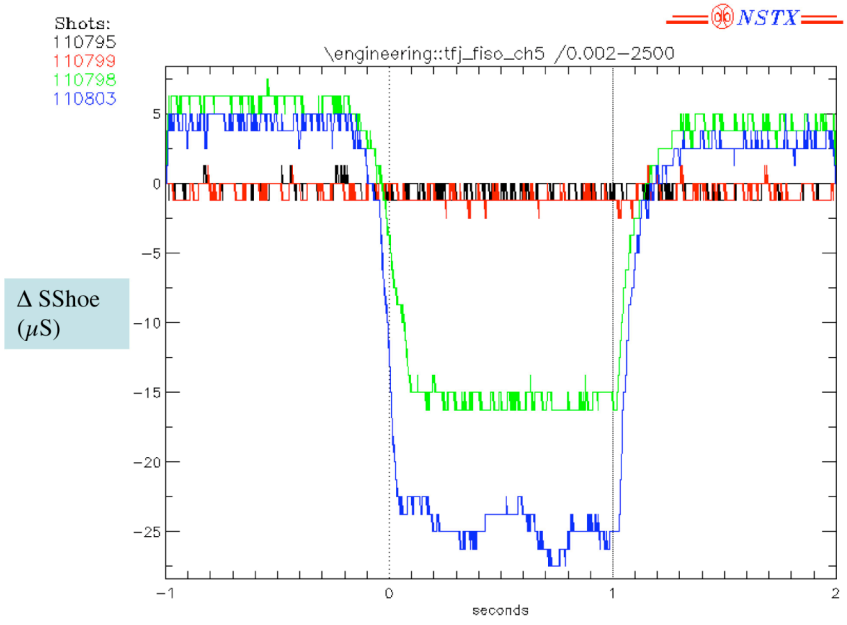

Figure 14 – Shear Shoe Strain Response

Response of the axial displacement to the combined field shots is shown in figure 15. Additional effects due to the operation of the OH and PF systems are noted.

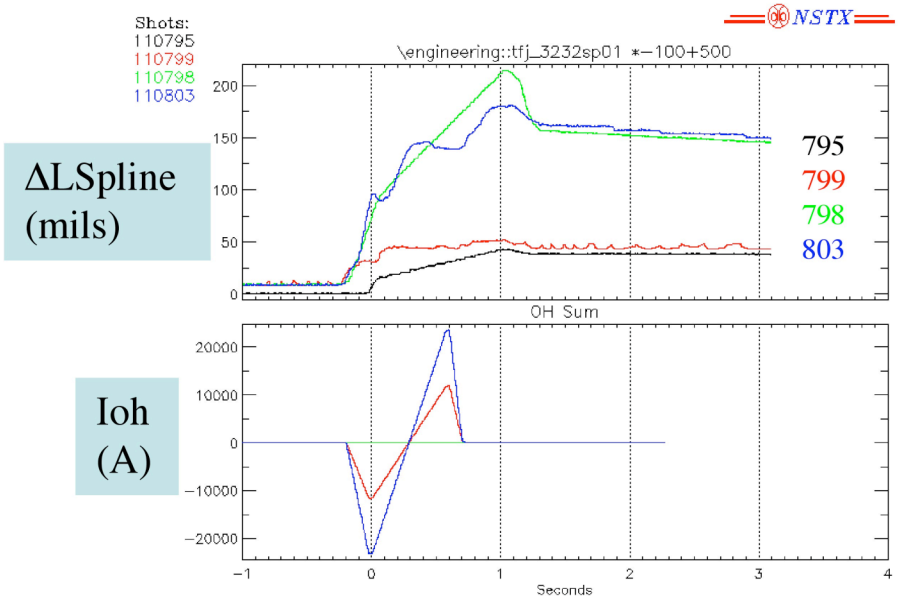

Figure 15 – Axial Displacement with Combined Field Loading

Figure 16 shows an overlay between the nominal combined field shot (110803) and another subsequent shot (110809) during which an OH fault occurred, and a rapid shutdown of the OH took place. It is postulated that the OH drives eddy currents in the umbrella cover such that, when the OH current is decreasing in magnitude, an attractive force is developed between the coil and the cover, causing a downward deflection. Then, when the current stops (and its derivative goes to zero), the cover is released from the force and undergoes a mechanical vibration.

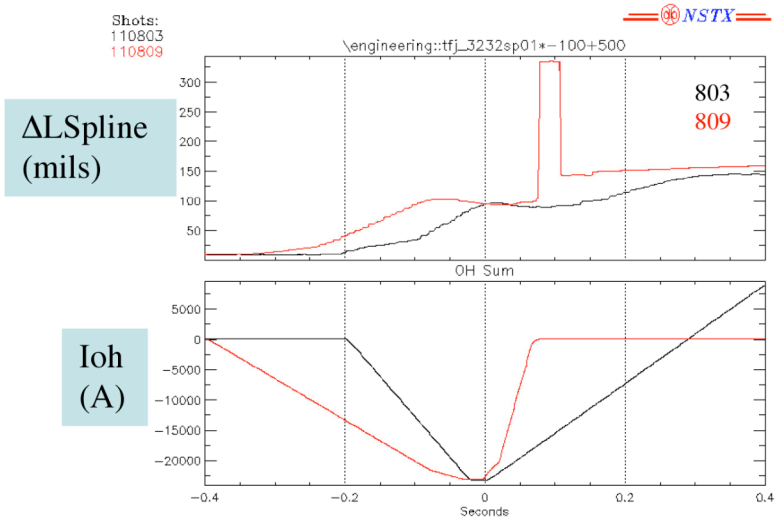

Figure 15 – Axial Displacement During OH Misoperation

Response of the angular twist at the end of flag TBD_TBD to the combined field shots is shown in figure 17. The twist during the pure in-plane shots is unexpected. The effect of the OH in the combined field shots is clearly evident.

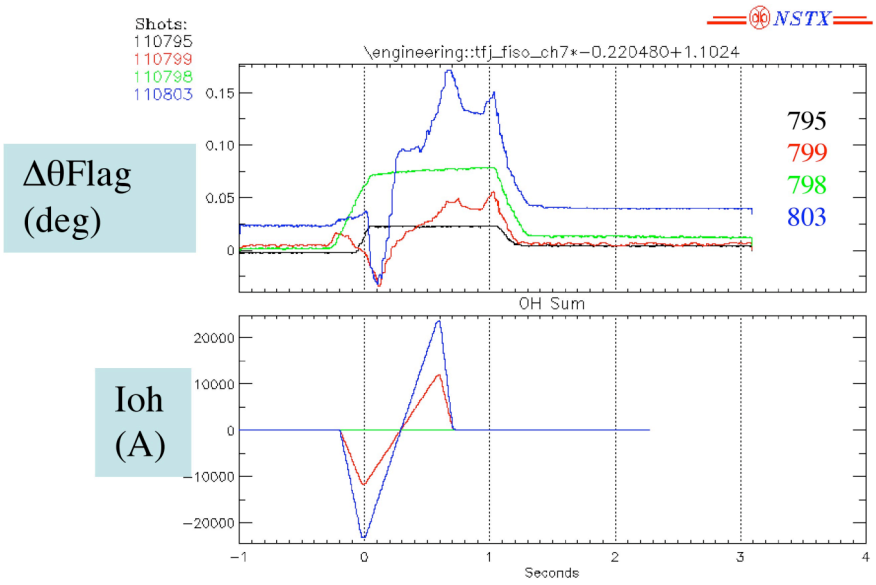

Figure 17 – Angular Twist of Outer Layer Flag

Comparison between Measurements and Analytic Predictions

Resistance

The measured resistance of 21_21 at the maximum time point, along with the minimum and maximum flag resistances at their maximum time points, is plotted in figure 18 for both the TF-only and combined field shots. The out-of-plane effect is noted. Also plotted are the predictions by Brooks of the resistance measurements at each side of the joint at 6kG. Unfortunately, at the present time, no ANSYS results are available for the resistance predictions for the ISTP shots.

While many of the joints appear to be on track toward the Brooks result for both the TF-only and combined field cases, many are exhibiting higher resistances and, in general, the out-of-plane effect seems to be higher than predicted.

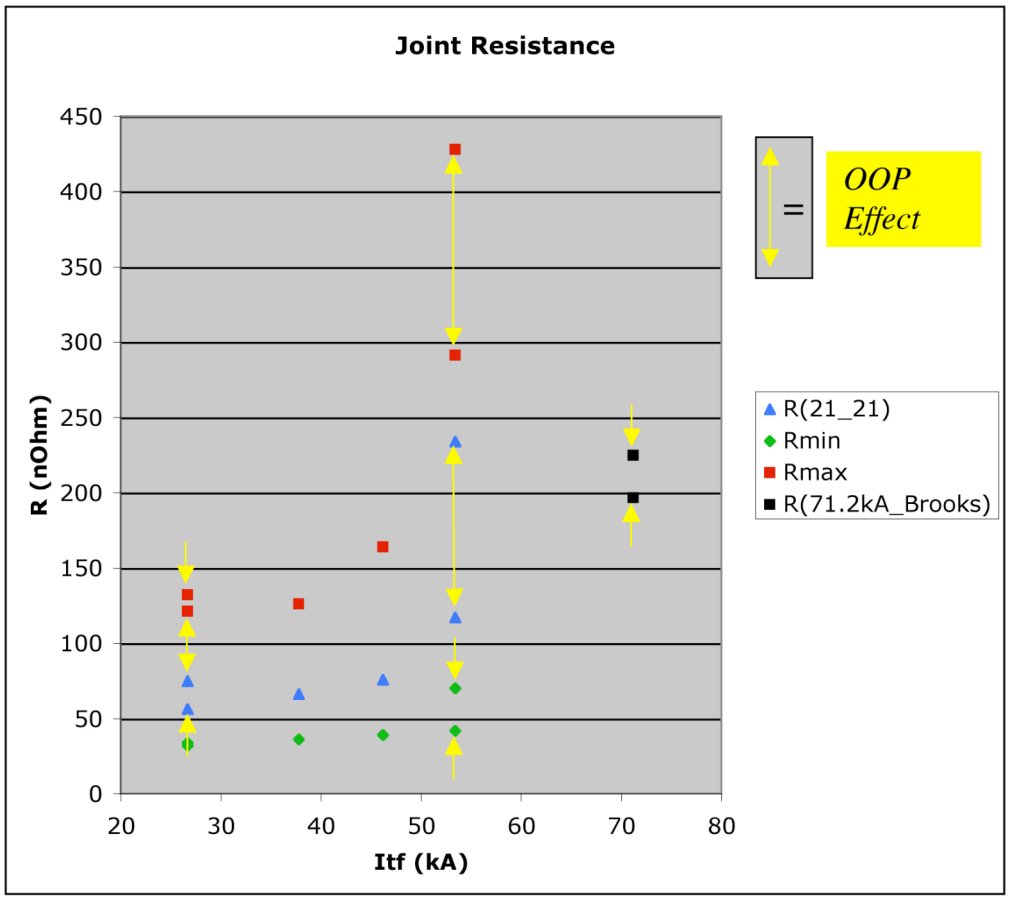

Figure 18 – Comparison of Resistance Measurements vs. Analysis

To give a sense of the variability in the joint behavior, figures 19 and 20 show the trend of resistance values for all of the joints at their maximum resistance time point during the ISTP tests. Also plotted is the value of TF current during each pulse. The translation between pulse number and shot number is given in the following table.

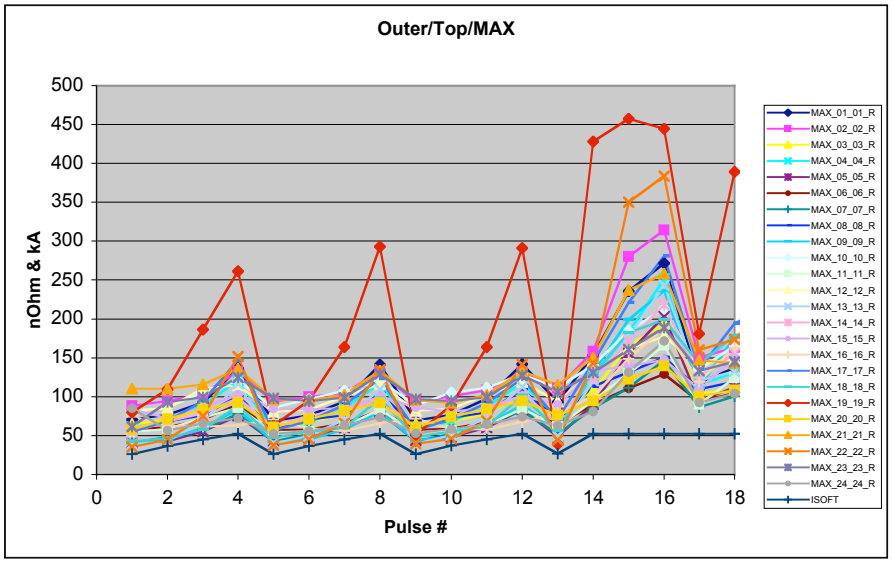

Figure 19 – Outer Top Resistances During ISTP at Maximum Time Points

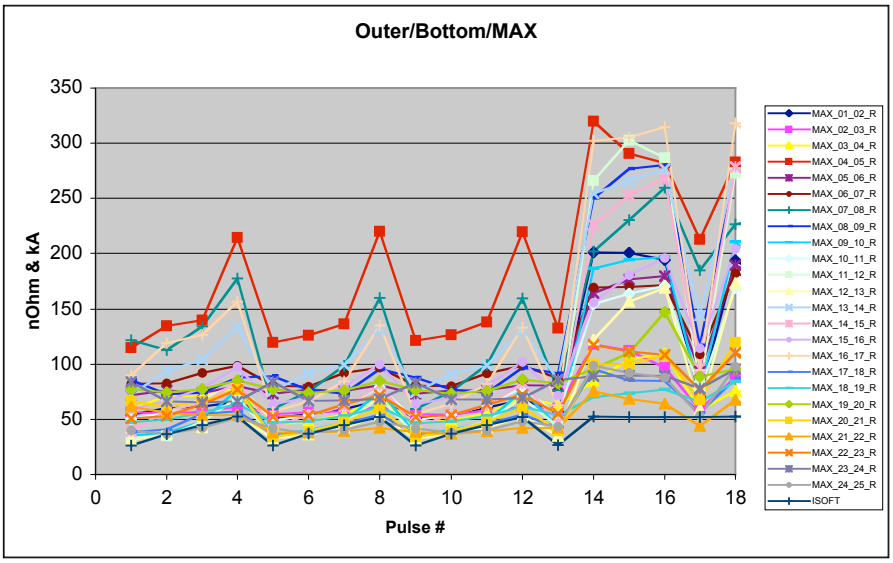

Figure 20 – Outer Bottom Resistances During ISTP at Maximum Time Points

TABLE 6 – SHOT NUMBERS IN FIGURES 19 & 20

Pulse #	Shot #
110795	9
110796	10
110797	11
110798	12
110799	13
110803	16

Temperature

Figure 21 shows the measured temperatures for the SOFT and EOFT conditions, versus the analytic predictions. Also shown is the adiabatic conductor temperature rise "Cond ΔT", and the maximum measured temperature rise "ΔT max" which occurred some time after the end of the pulse (refer to figure 7). The first discrepancy noted is that, for all pulse levels, the predicted ΔT EOFT is much higher than measured. The second discrepancy is the fall-off in the measured ΔT EOFT at the highest pulse level. Possible explanations for these discrepancies are as follows. First, the contact thermal resistance used in the thermal model was based on engineering judgment, not on any sort of measurement. Second, the contact thermal resistance in the model was not varied as a function of pressure along the joint. Third, it appears that significant pressure redistribution is occurring at a lower level of B_t than predicted by the model. This would lead to a current redistribution, and a relocation of the hot spot away from the vicinity of the temperature probe.

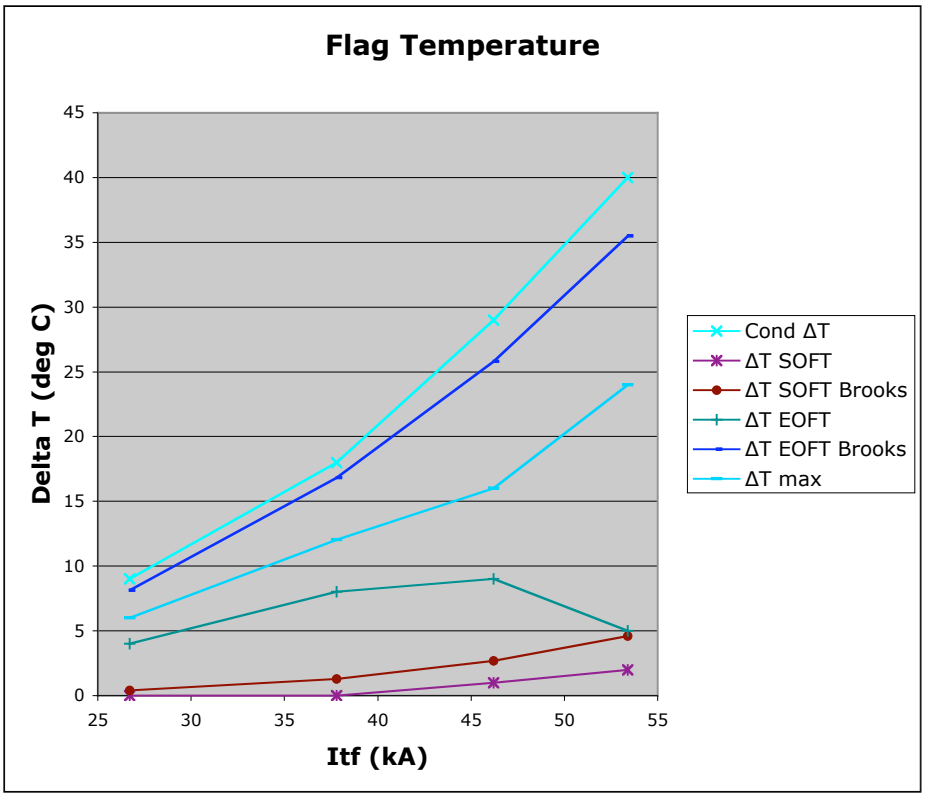

Figure 21 – Comparison of Temperature Measurements with Analysis

Strain

Figure 22 shows the measured flag strains for the SOFT and EOFT conditions for TF-only pulses, versus the analytic predictions. The predictions are relatively close, up to the final shot. Again, the effect of pressure and current redistribution and lower local temperature is also seen in the strain signal, which is significantly effected by temperature.

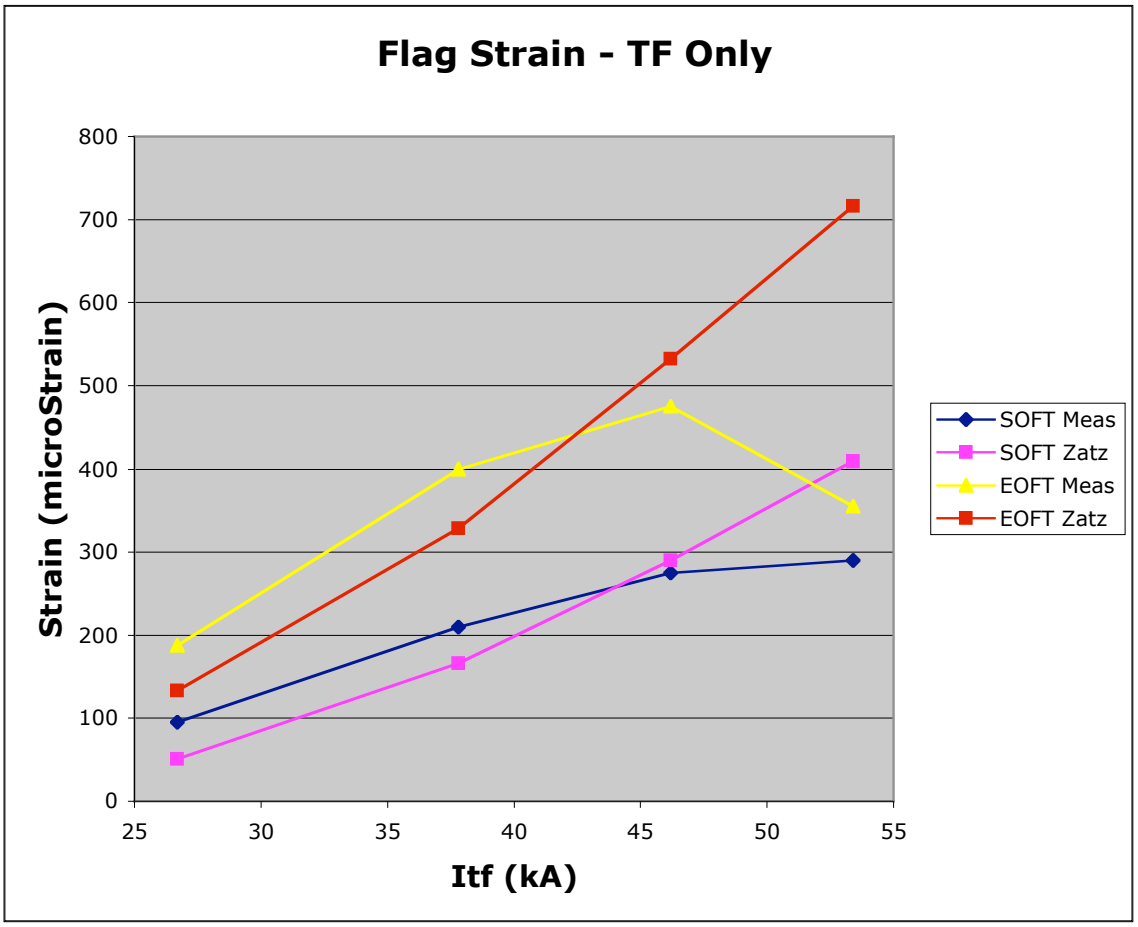

Figure 22 – Comparison of Flag Strain Measurements with Analysis

Figure 23 shows the measured shear shoe strain for the SOFT and EOFT conditions for TF-only pulses, versus the analytic predictions. The predictions are higher than the measurements at the low field levels, and lower at the high field levels. This suggests that the shear shoe is taking less load and the low field levels, and more at the high levels.

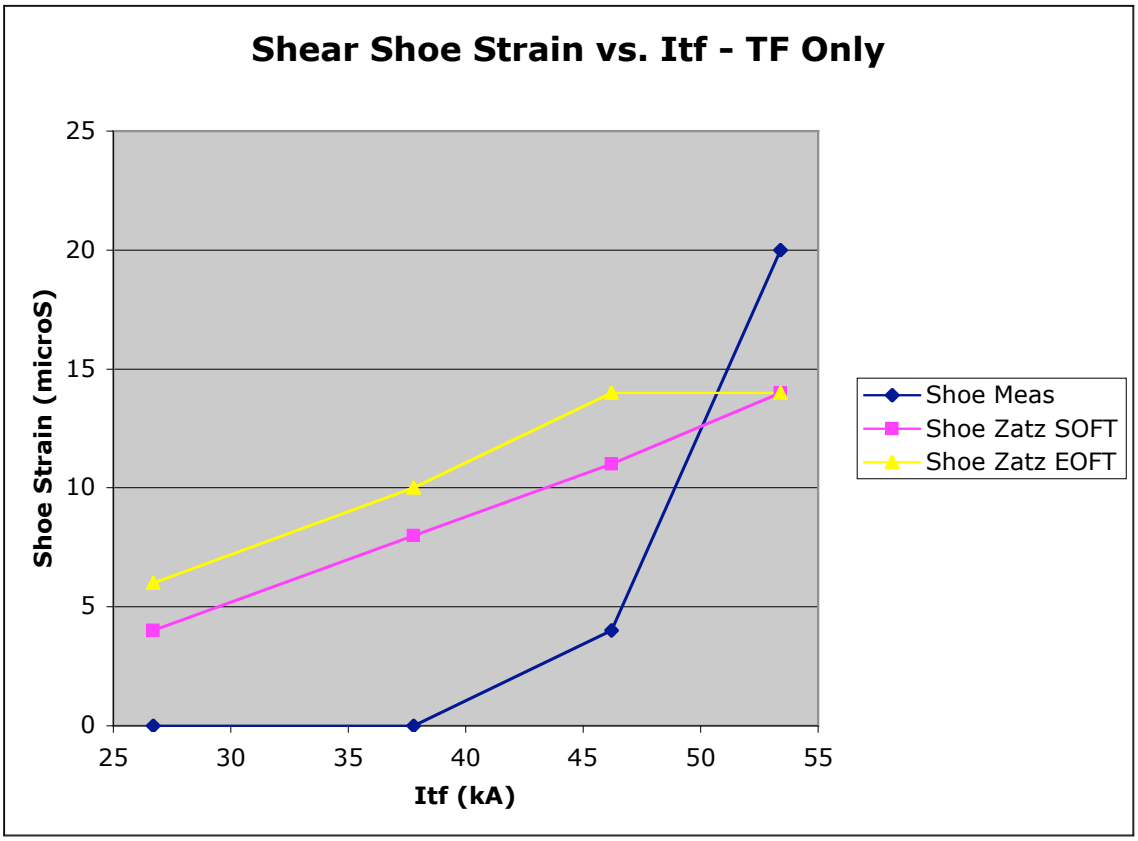

Figure 23 – Comparison of Shear Shoe Strain Measurements with Analysis

Figure 24 shows the measured flag strain for the SOFT, OHSS (OH second swing) and EOFT conditions for the combined field pulses, versus the analytic predictions, for the "A" and "B" probes on either side of the flag. The largest discrepancy here relates to the out-of-plane effect on strain which the analytic model seems to overestimate. This is surprising because it is contradictory to the prior observation that the out-of-plane effect on resistance appears to be larger than predicted.

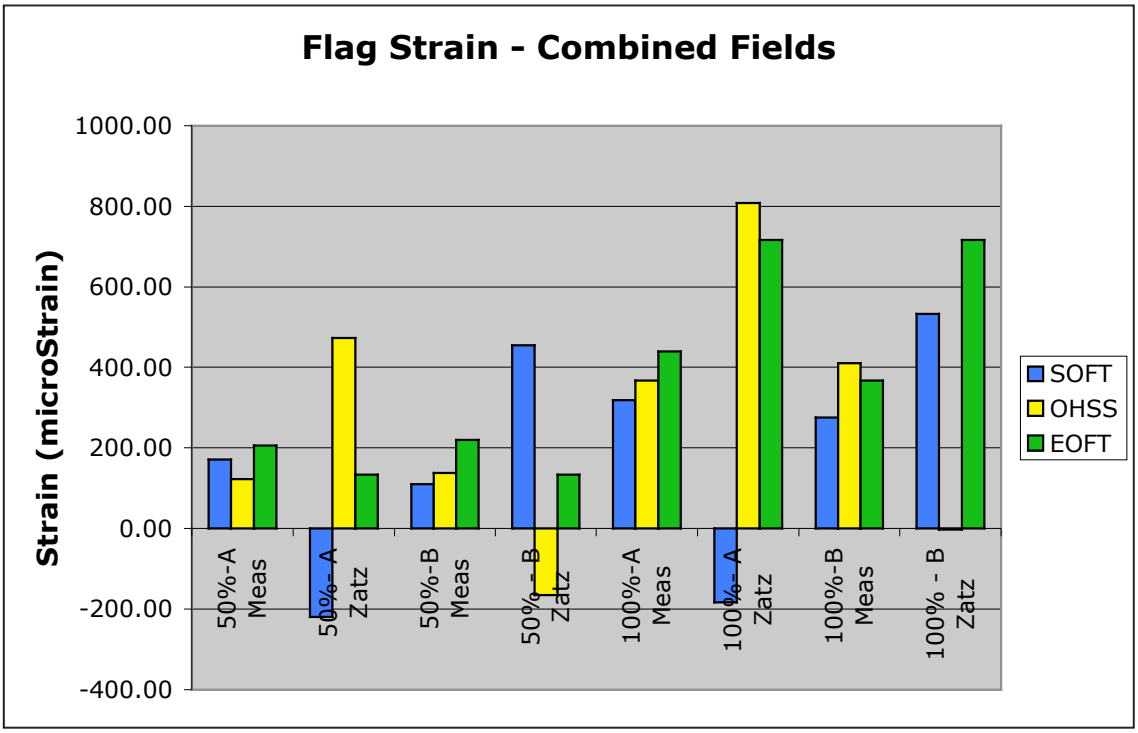

Figure 24 – Comparison of Flag Strain Measurements with Analysis

Displacement

Figure 25 shows the measured axial displacement versus the analytic predictions. This shows the predicted ΔL (DL(calc)), the ΔL measured at the end of the TF flat top (see figure 10) when it was at its peak value (DL(meas:peak), and the ΔL measured after the TF was off at the start of the thermal decay (DL(meas:decay). Also shown is the difference between the ΔL values before and after the TF current turns off and the EM effects disappear. Finally, the DL(EM) curve shows the ΔL calculated for the TF bundle based on the tension arising from the in-plane EM load developed by the flags. It is clear that this effect explains the dip in the displacement curve following the shutdown of the current, and validates the calculation of the force on the flags. Furthermore, the ΔL values during the decay match the values predicted based on thermal effects alone, which gives a nice verification of the temperature rise modeling.

The calculation basis for the elastic deformation of the TF bundle is given in Table 7.

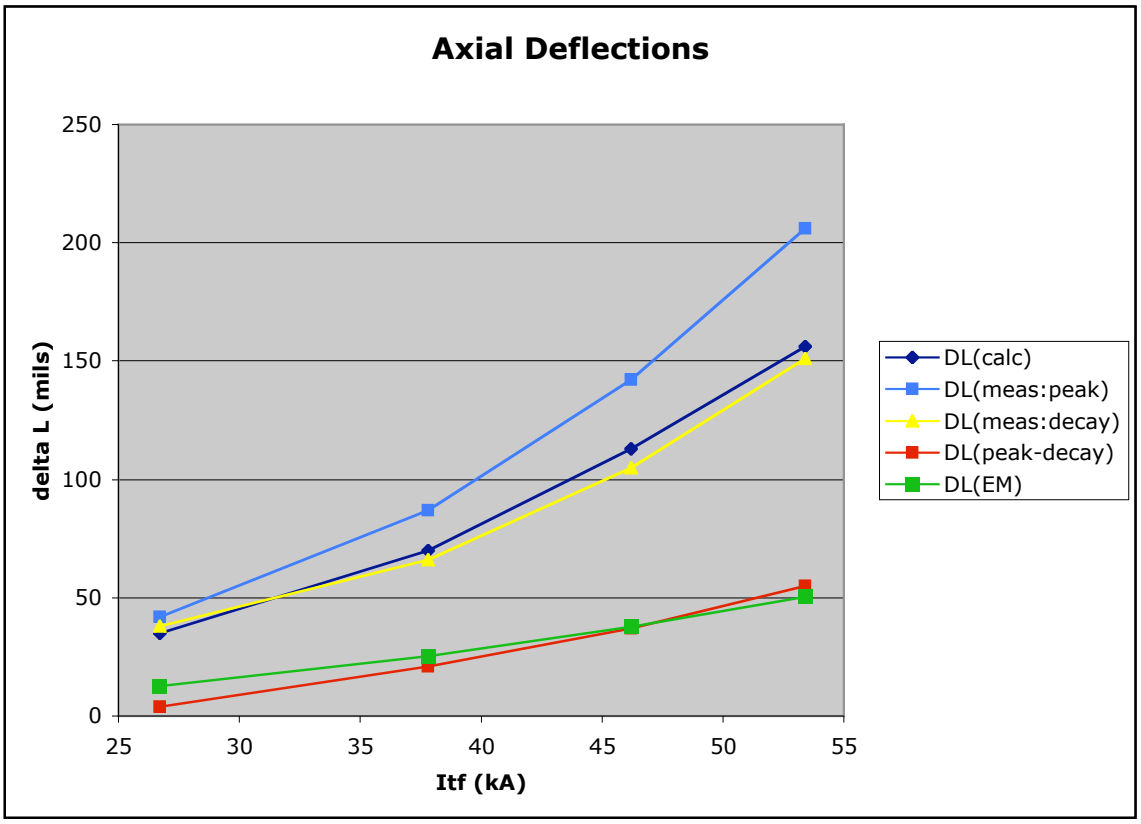

Figure 25 – Comparison Axial Displacement Measurements with Analysis

TABLE 7 – CALCULATION OF TF BUNDLE ELASTIC DEFORMATION

Itf	26.7	37.8	46.2	53.4	kA
Fv/outer flag	1299	2603	3888	5194	lbf
Fv/inner flag	325	651	972	1299	lbf
Total Fv	35061	70273	104976	140245	lbf
Copper Modulus	1.7E+07	1.7E+07	1.7E+07	1.7E+07	psi
Copper CSA	37.8	37.8	37.8	37.8	in^2
L	231.0	231.0	231.0	231.0	in
ΔL Pulse (EM)	0.013	0.025	0.038	0.050	in

Figure 26 shows the measured axial displacement versus the analytic predictions. This indicates a somewhat greater twist than assumed. After additional measurements are made of the inner flag end twist, consideration should be given to adjusting the modeled stiffness of the spline/outer VV load path to reflect this result.

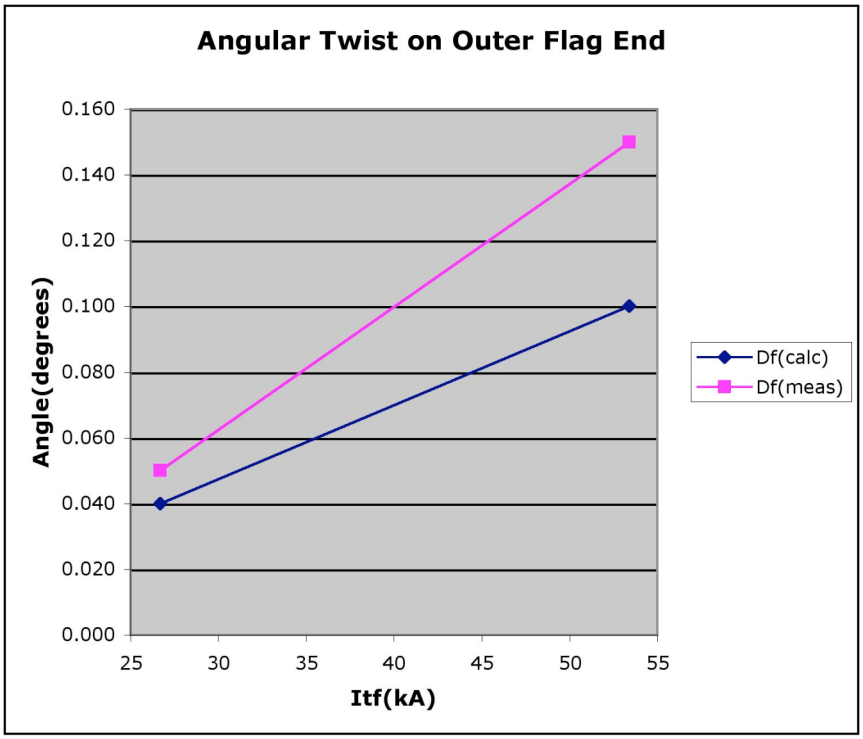

Figure 26 – Comparison Axial Displacement Measurements with Analysis

Trends

In order to trend the resistance measurements, three 50mS averaging intervals were established as shown in figure 27. The SOP "pedestal" is a 5kA interval during which no PF loads are on, and as such provides a measurement of the joint resistance with relatively low EM loads at the beginning of every pulse. The SOFT interval corresponds to a time point when full EM loads, including the OH, are typically applied, but when the TF bundle has not experienced very much heating. The EOFT interval corresponds to the end of flat top when the OH and other PF coils are typically off, but at which time most of the coil heating has occurred. So, each averaging interval gives a somewhat different view of the performance of the joint.

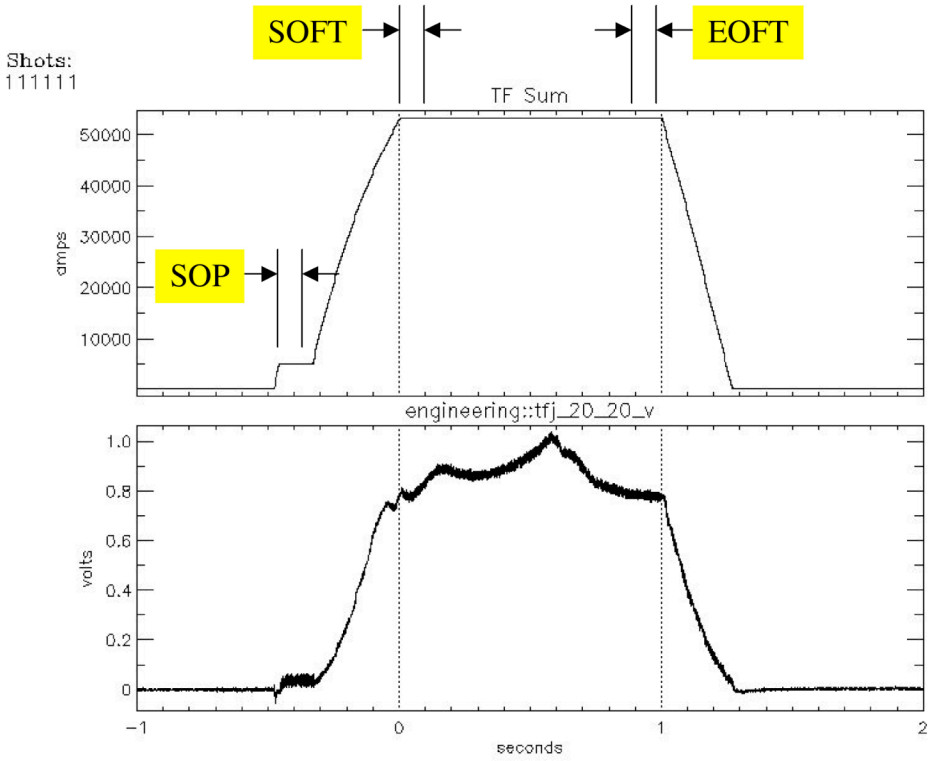

Figure 27 – TF Resistance Averaging Intervals

The resistance during each of these intervals is automatically calculated every pulse and stored in a database. This is in addition to the 200A measurements which are made manually at the discretion of the operations team. The results for the prior 200 shot numbers as of 2/12/04 (around 160 pulses with TF current), shown in figures 28-43, demonstrate that the condition of the joints is basically stable. Note that the level of TF current is also plotted for the pulse measurements. The effect of the TF current level on the resistance measurement is clearly evident. Some timing and algorithm problems are evident in the earlier shots but these issues have now been resolved as evidenced in the later shots.

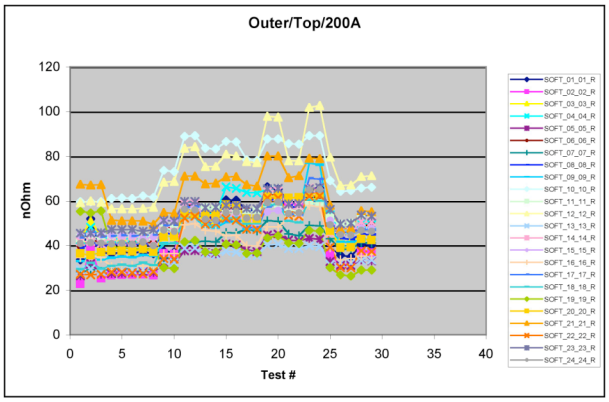

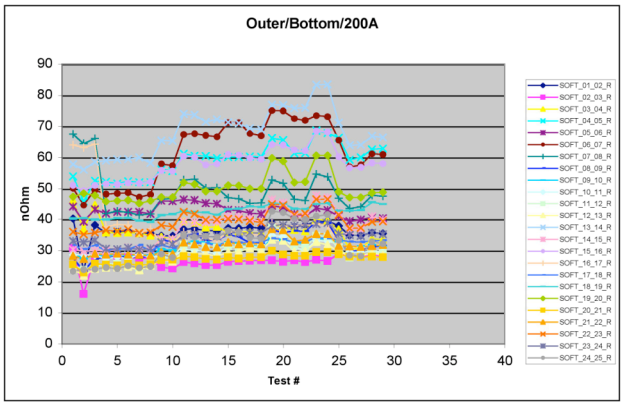

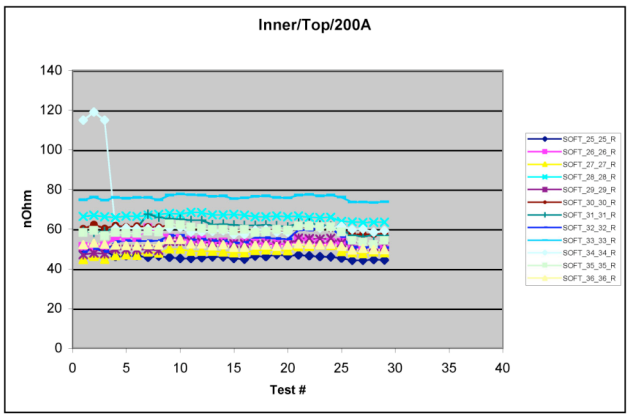

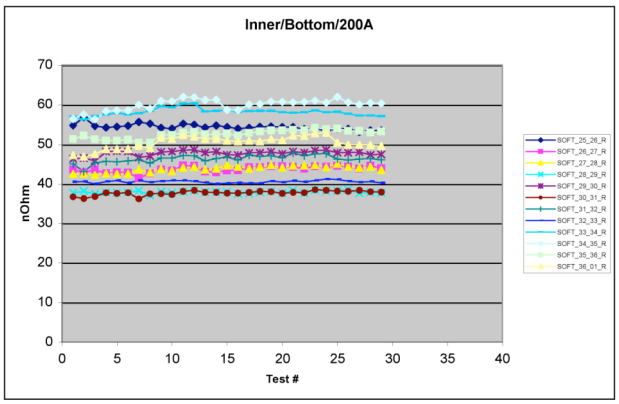

Figure 28 – 200A Trends

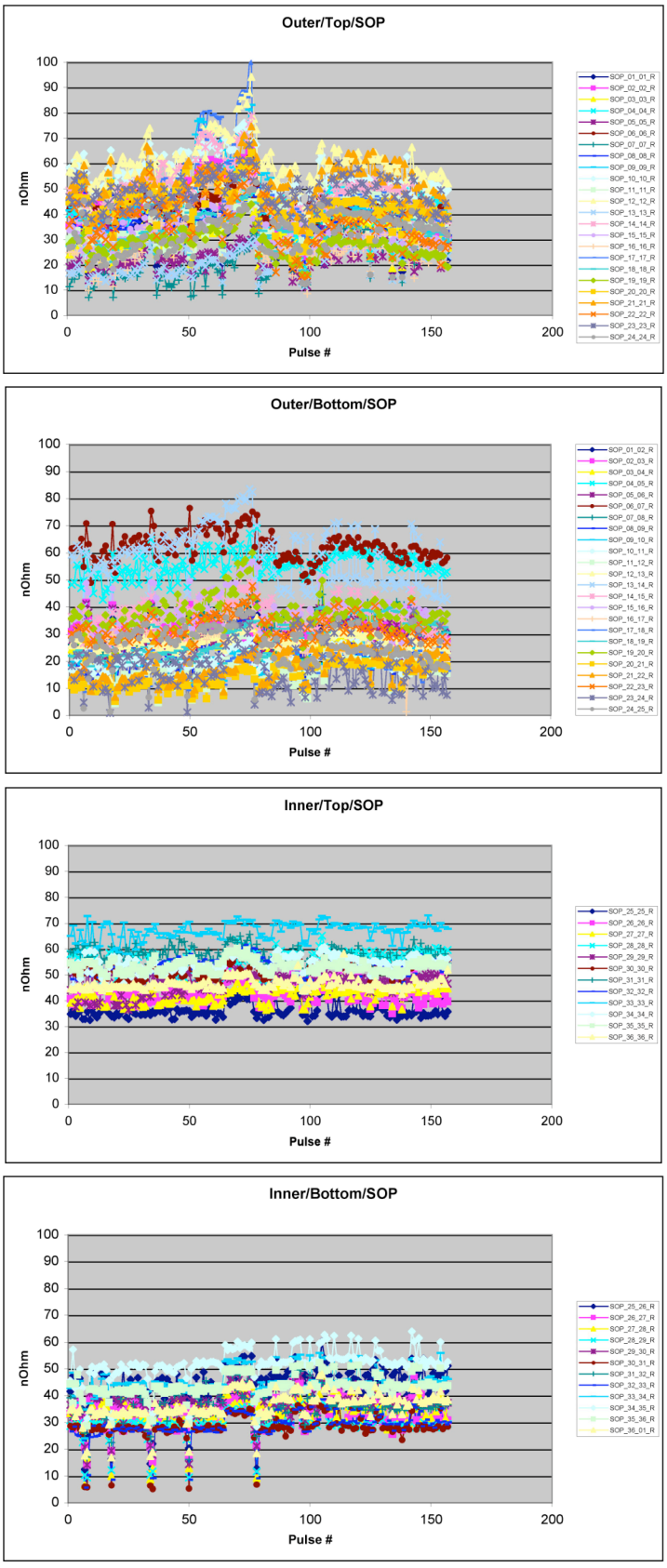

Figure 29 – SOP Trends

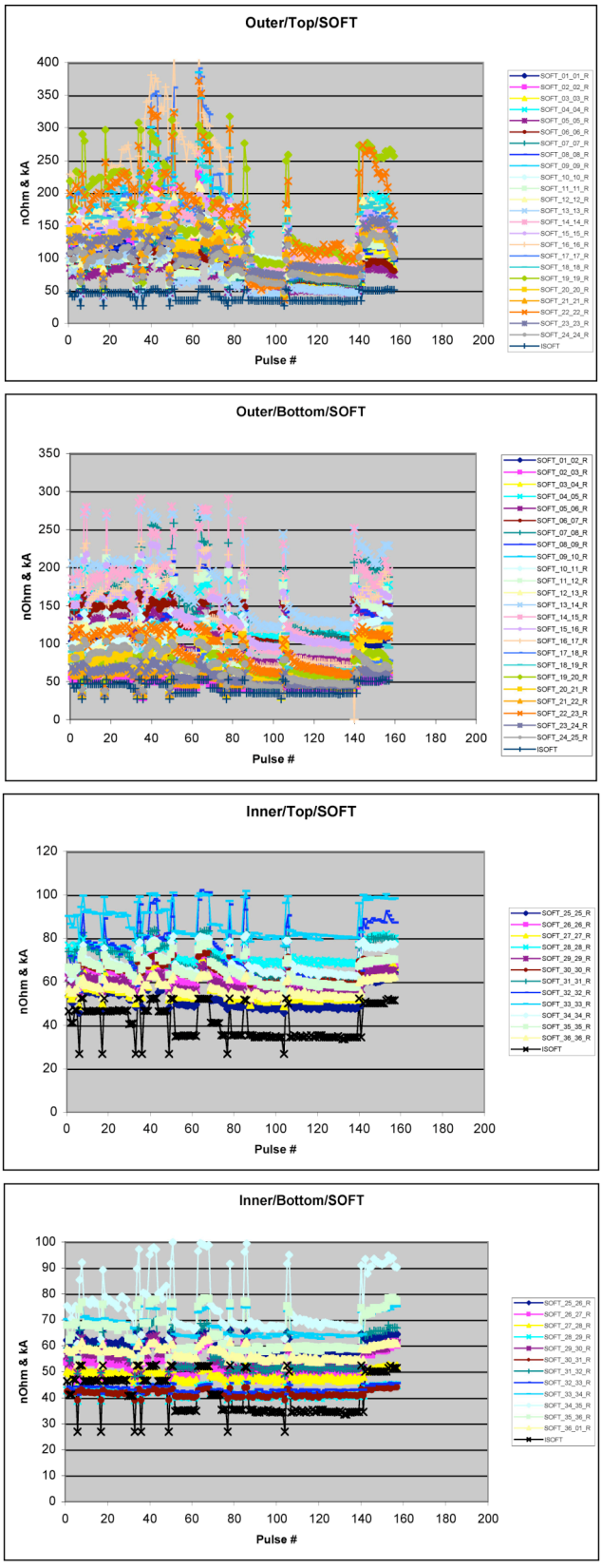

Figure 30 – SOFT Trends

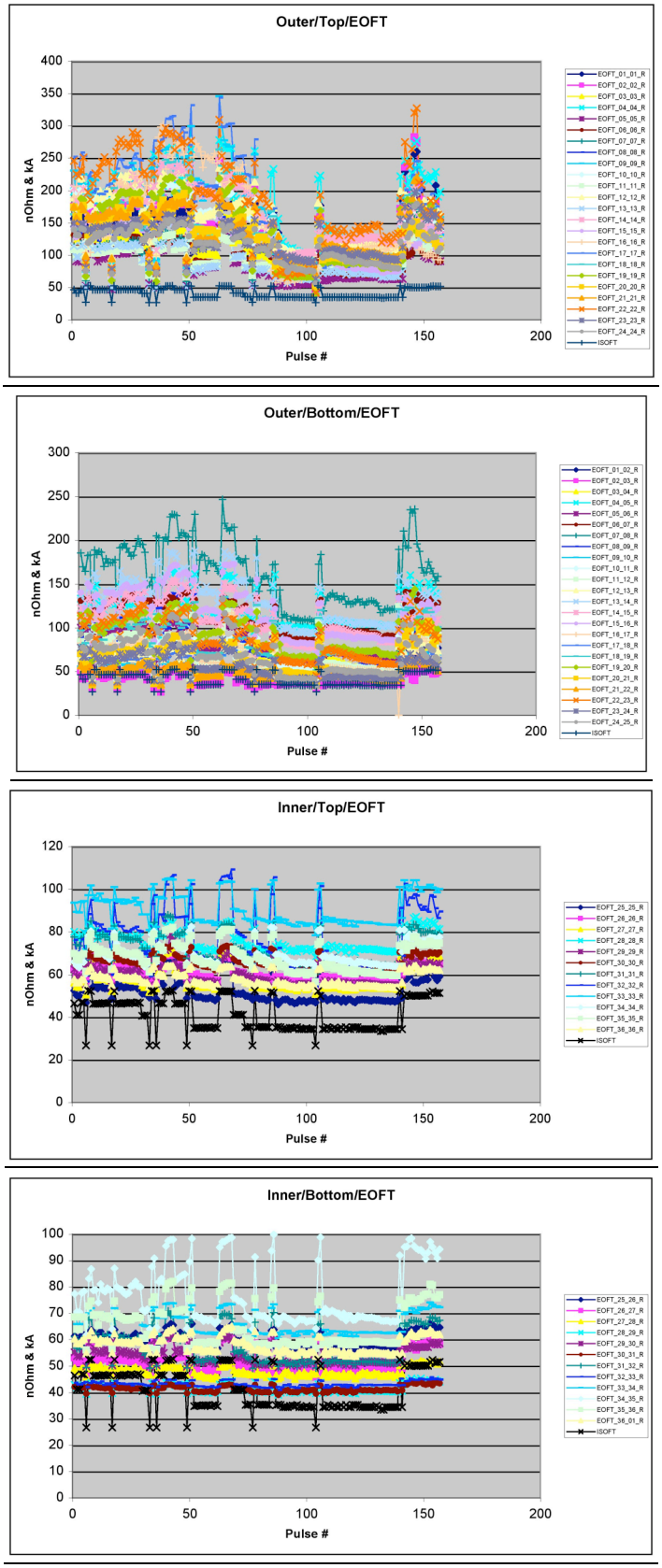

Figure 31 – EOFT Trends

Careful evaluation of these results indicates that the relative goodness or badness of the various joints depends on the condition at the time of measurement. For example, the distribution during the 200A test is similar to that during the SOP measurement, but different than that during the SOFT and EOFT measurements.

The joints which typically exhibit the most resistance during the pulse (SOFT and EOFT) are 16_16, 17_17, and 22_22, all outer layer flags on the top of the machine. Also, joint 19_19 exhibited relatively high resistance early on. The tension on its studs was checked on 2/8 and found to be normal. Since then, however, its resistance has been relatively good.

Figure 32 shows the resistance as measured by the two probes on 22_22 (both sides are instrumented) along with the energy = $\int I(t)v(t)dt$ of the highest of the two during a 100% test shot (typically worst case condition). This result shows a dissipated energy of order 1.2kJoule across the joint, corresponding to an average resistance of order 1.2e3J/3.5e9A^2-sec = 340nΩ.

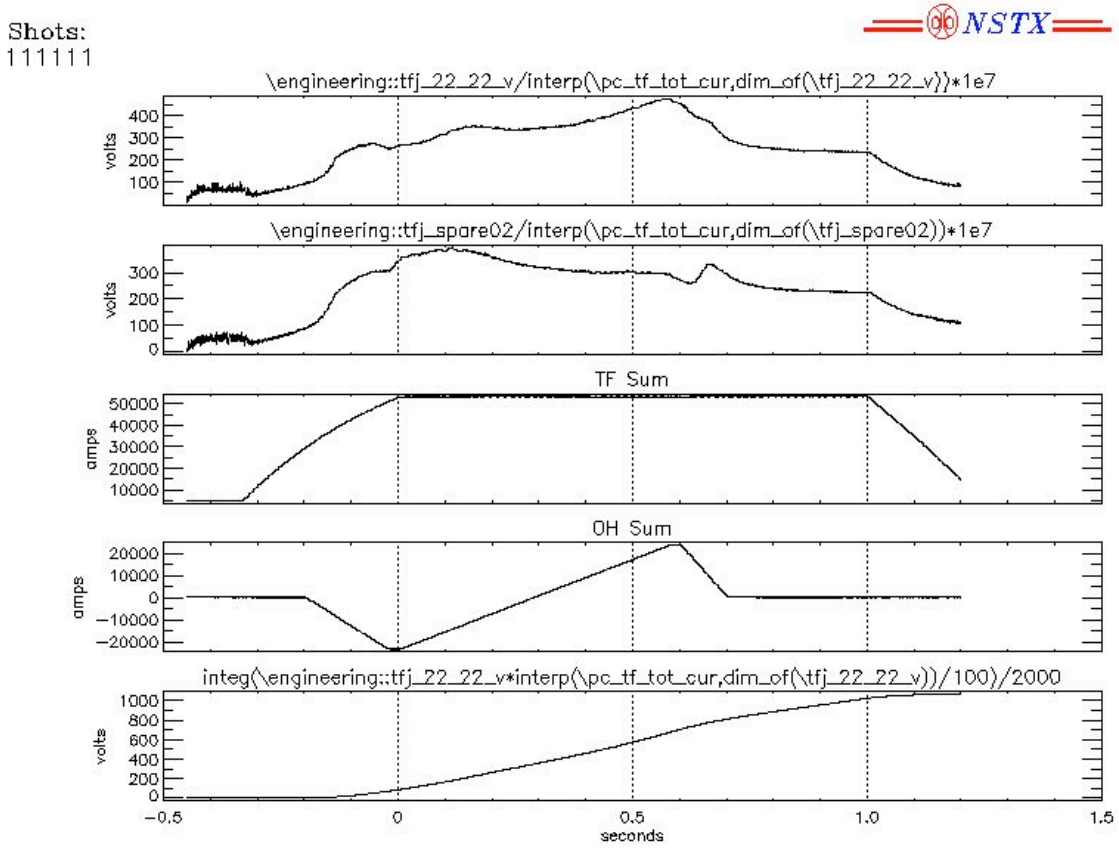

Figure 32 – EOFT Trends

This level of dissipation is slightly less than that assumed in the analysis by Brooks, where the flat top resistance on the worst side of the joint was equal to 225nΩ and the $\int i^2(t)dt$ of the total pulse was 6.5e9A^2-sec, and the total dissipation then $\int i^2(t)dt*R$=1.46kJ. From this result one can conclude that the present nominal operating condition dissipates

a bit less energy than in the Brooks analysis[3], and that a worst case fault (Level 1 fault at end of 1.0sec flat top at 4.5kG) would dissipate a bit more. However, it must be kept in mind that this is an approximate result since the $\int i^2(t)dt$ during L/R decay has less of an impact than that during flat top when the field is high and the resistance is high. In any case, see the following table.

TABLE 8 – DISSIPATION AT TF JOINT

	6kG Brooks	Present 4.5kG Nominal	Present 4.5kG Worst Case	
I2T	6500.0	3500.0	5000.0	kA^2-sec
R	225.0	340.0	340.0	nOhm
W	1462.5	1190.0	1700.0	Joule

Conclusions

Some aspects of the measurements are in agreement with the predictions, but others are not.

Follow-on efforts will be necessary to refine and benchmark the analytic models so that performance can be better assessed and we can justify going to higher TF levels.

The variability in joint resistance is higher than expected.

The worst case joints appear to be dissipating approximately the same amount of energy at 4.5kG as was allocated in the analysis for the 6kG case. On this basis, along with the evidence that stable conditions have been achieved, continued operation with the present restrictions is considered to be safe.

Whether or not this is a serious issue needs to be assessed by the analysis. It may well be that pressure redistribution and its effect on resistance distribution simply shifts the current pattern in such a way that hot spot temperatures are not significantly increased. This needs to be determined by analysis prior to proceeding to higher operating levels.

[3] "TF Electrical Joint Analysis", NSTX-CALC-13-5-1, A. Brooks